International Journal of
Advanced Thermofluid Research

ISSN 2455-1368
www.ijatr.org

Photocurrent, Absorption and Electrochemical Impedance Analyses on Strontium Titanate Ferrate Films for Solar Energy Conversion

Ibrahim A. I. Hassan

Department of Chemistry, University of Bath, Bath, BA2 7AY, UK.
Department of Chemistry, Faculty of Science, South Valley University, 83523 Qena, Egypt.

Keywords
Solar Cells •
Perovskite •
Water Splitting •
Solid Solution •
Solar Energy Conversion •
Strontium titanate ferrate •
Spray Pyrolysis •
Renewable Energy •
UV-vis.

Abstract

This article presents photon to electricity conversion analysis, and absorption and impedance measurements, on a new class of solid solutions, known as $SrTi_{1-x}Fe_xO_{3-y}$ or strontium titanate ferrate (STF). Incident photon-to-current efficiency (IPCE), UV-vis absorption spectroscopy and electrochemical impedance spectroscopy (EIS) were performed. The STF samples were prepared by employing spray pyrolysis approach on ITO substrates, at high temperature. A Varian Cary 50 Probe spectrometer was used for UV-vis measurements, and EIS results were obtained by using Z-plot software. In general, the proposed nanostructured STF films show good photoactivity properties giving high photocurrent response and with IPCEs of up to 11%. The samples show high absorption of UV-visible light in air, in the wavelength range 300 to 400 nm. The IPCE data suggest good photoelectrochemical activity, and the IPCE increases slightly with increase in the film thickness. Furthermore, the impedance is found to increase with increase in the applied potential and to decrease with the increase in film thickness.

Received Oct 28, 2015 **Revised** Nov 26, 2015 **Accepted** Nov 25, 2015 **Published** Dec 01, 2015

***Corresponding email**: I.Hassan@bath.edu (Ibrahim A. I. Hassan).

DOI: https://doi.org/10.51141//IJATR.2015.1.2.2

1. Introduction

Mixed metal oxides can be employed to control and improve physical properties, for example, for photo-electrochemical films. For the case of iron oxides it has been shown that strontium ferrites and strontium titanates could form solid solutions to provide control over ionic and electronic conductivity (Brixner, 1968). Mixed ionic electronic conductors (MIEC) play a core role in the manufacturing of solid-state electrochemical devices, which can be designed for energy conversion and for gas sensor applications (Rothschild and Tuller, 2006). There are many important applications for MIEC such as solid oxide fuel cell (SOFC) electrodes, oxygen separation membranes,

insertion electrodes, electrochromic windows, oxygen and gas sensors, and as catalysts (Rothschild et al., 2006). The strontium titanate ferrate (STF) family ($SrTi_{1-x}Fe_xO_{3-y}$) forms a continuous solid solution between strontium titanate ($SrTiO_3$) and strontium ferrite ($SrFeO_3$) over the entire composition range $0 < x < 1$. $SrTi_{1-x}Fe_xO_{3-y}$ (STF) solid solution materials have been prepared (Rothschild et al., 2006) by conventional mixed-oxide techniques and by calcination of $SrCO_3$, Ti, Fe mixed oxide in air at 1200^0C. The electronic structure, defect chemistry and transport properties of its members have been studied (Rothschild et al., 2006).

The related titania-doped Ruddlesden-popper ferrite ($Sr_3Fe_{2-x}Ti_xO_{6+\delta}$) where; $0 < x < 2$, have been prepared and characterized (Brixner, 1968). This material has been prepared by conventional solid-state reaction method starting with Sr, Ti, and Fe pure oxides. After pressing the metal oxides mixture into discs under high pressure, high temperatures up to 1350 ^{0}C have been used to prepare these materials. The characterization has been reported by XRD and thermogravimetry measurements. The effect of oxygen content and titania- doping have been studied. The oxygen ion conductivity was found to decrease with increasing the titania content.

In the present work, STF-like films are prepared and investigated for photo-electrochemical applications. After failing to keep the conducting part of ITO quartz slides without damage by the effect of the very high calcination temperature 1200^0C, a low temperature approach has been investigated. STF films are prepared on ITO conducting glass by normal spray pyrolysis technique at 500^0C and via annealing in air at the same temperature for 2 hours in a furnace. Structural studies are preliminary and in-conclusive, but initial photoelectrochemical studies have revealed very promising photo-activity for water splitting.

2. Materials and Methods

2.1 Chemical Reagents

0.2 M $Fe(NO_3)_3.9H_2O$ 99.999% (Sigma-Aldrich) / MeOH, 0.1 M $Sr(NO_3)_2$ 99.995% (Aldrich) / H_2O, di-isopropxytitanium-bis-(acetylacetonate) (C_{16} H_{28} O_6 Ti) solution, 75% wt.% (Aldrich) / isopropanol precursors have been prepared. All chemicals were obtained commercially and used without any further purification.

2.2 Instrumentation and Measurements

An Auto-lab potentiostat (Ecochemie) was employed in three-electrode configuration. Incident photon-to-current efficiency (IPCE), UV-vis absorption spectroscopy and electrochemical impedance spectroscopy (EIS) were performed. A hotplate, a sonicator, and a furnace instrument were used for film preparation. A Varian Cary 50 Probe spectrometer was used for UV-vis measurements. To measure EIS, the Z-plot software was used to operate a Solartron SI 1286 electrochemical interface and a Solartron SI 1260 impedance / gain-phase analyser.

The IPCE experiments were carried out using the experimental setup shown in Figure 1. Output photocurrent from the cell, detected with the aid of chopped light and a lock-in amplifier, was plotted as a function of wavelength of incident light. The applied wavelength was varied from 550

nm to 300 nm in steps of 10 nm. The scan parameters used for all IPCE measurements are given in Table 1.

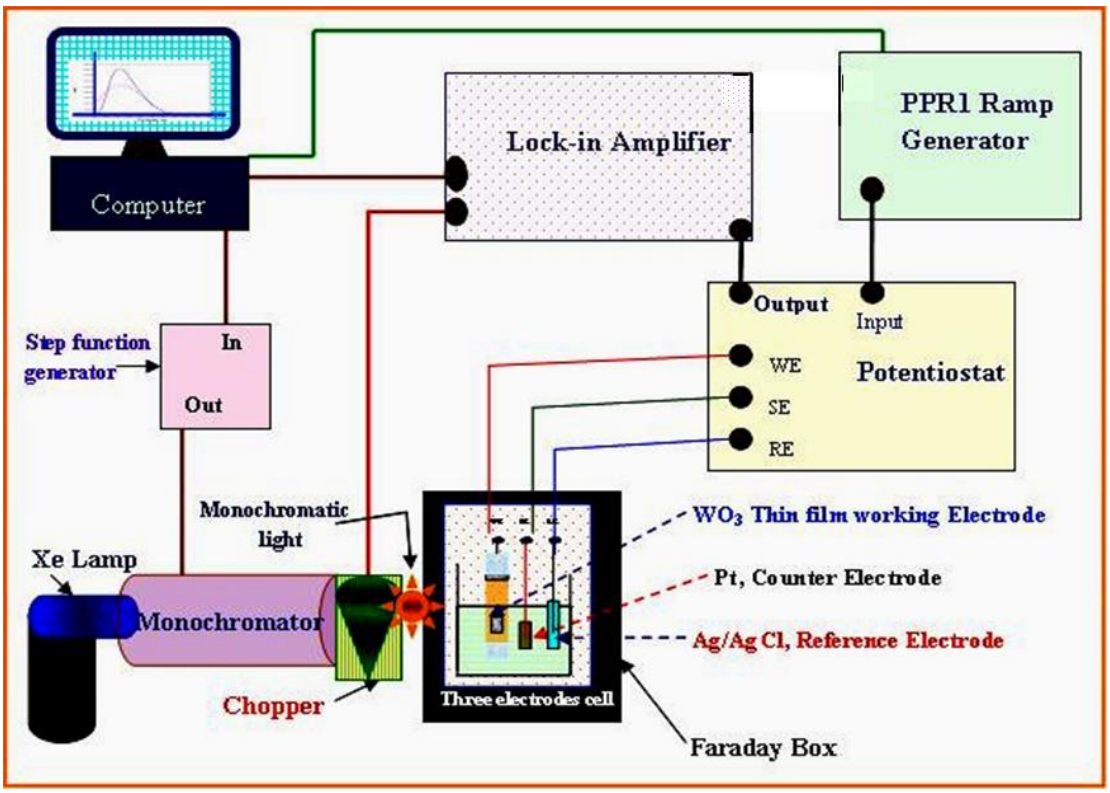

Figure 1. Experimental setup for incident photon to current efficiency (IPCE) experiments.

Table 1. The scan parameters used in IPCE measurements

Delay time	Measurement time	Delay Time	Chopping frequency
1 s	3 s	3 s	73 Hz

The specific apparatus for IPCE measurements was based on a Stanford Research Systems SR830 lock-in amplifier, an Amko SMD 101-M stepping motor control, a home-made potentiostat, an Amko A1020 75 W xenon lamp powered by an LPS75X/2 supply, an Amko monochromator with 10 nm spectral resolution, and 2.5 nm input/output slits on the 0.6l B - 1.6l B setting. The PPR1 generator was used to maintain a specific potential in which a strong photocurrent response is observed.

IPCE data were recorded for each sample with both EE (Electrolyte-Electrode or front) and SE (Substrate-Electrode or back) illumination. The wavelength dependence of the current from a

silicon photodiode of known IPCE (Hassan, 2015) function was measured to allow the calculation of $IPCE_{cell}$ via Equation (1). Figure 2 illustrates the illumination via EE and SE sides of a WO_3 film, as an example.

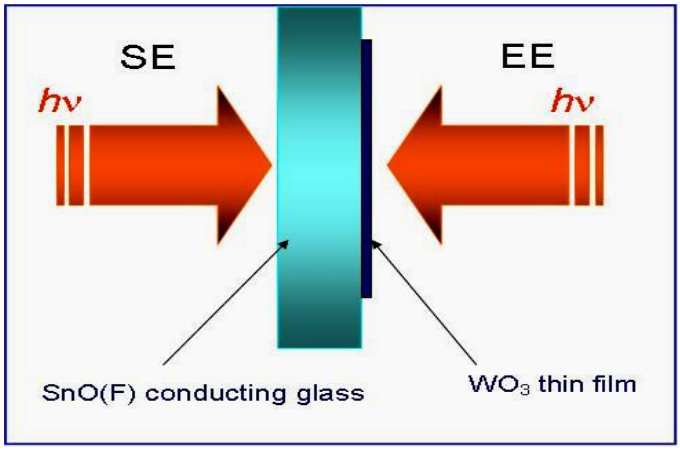

Figure 2. EE and SE illumination of the semiconductor WO_3 electrode as an example for investigated nanostructured films.

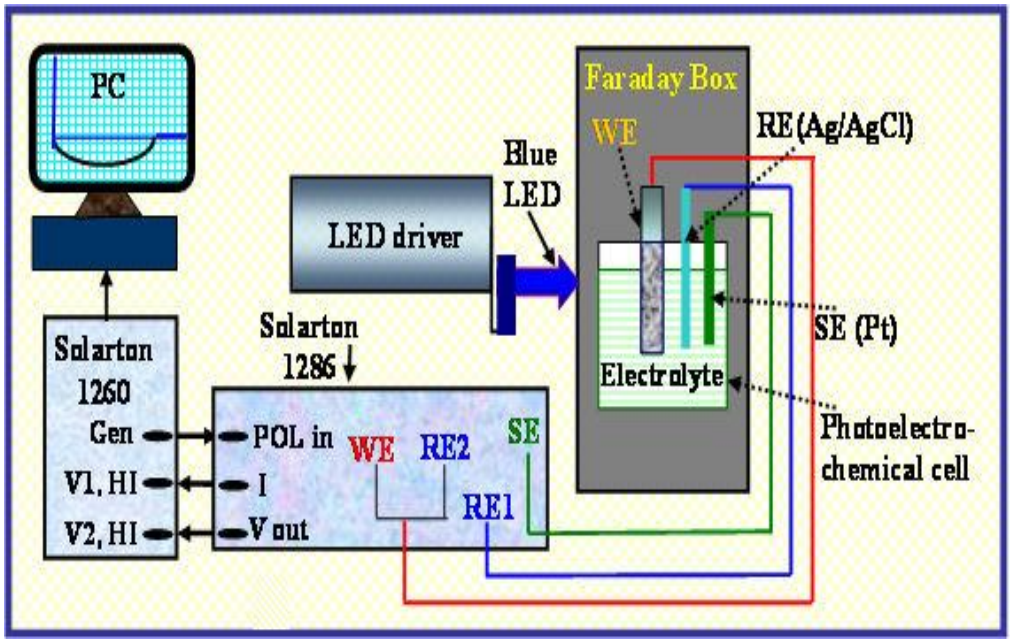

Figure 3. Experimental setup for electrochemical impedance measurements.

$$IPCE_{cell} = \frac{i_{cell}}{i_{pd}} IPCE_{pd} \quad (1)$$

Here i_{cell} is the photocurrent of the electrode under investigation cell and i_{pd} is that for the standard photodiode. The $IPCE_{pd}$ is a standard known value used for calibration and this therefore allows the $IPCE_{cell}$ to be calculated. Figure 3 shows the experimental setup used for EIS measurements. The SI 1286 applied a dc potential and an AC potential to the cell with 10mV amplitude from, SI 1260. The frequency was scanned over different frequency ranges according to the investigated films. The dc potential bias was defined to correspond to the open-circuit voltages of the dark or illuminated cell. The SI 1260 detected and measured the impedance of the cell.

3. Results and Discussion

3.1 Absorption Spectroscopy and IPCE Studies

STF samples showed high absorption of UV-visible light in air, in the wavelength range 300 to 400 nm (Figure 3). As expected, it was found that absorption increases with increasing the spraying time.

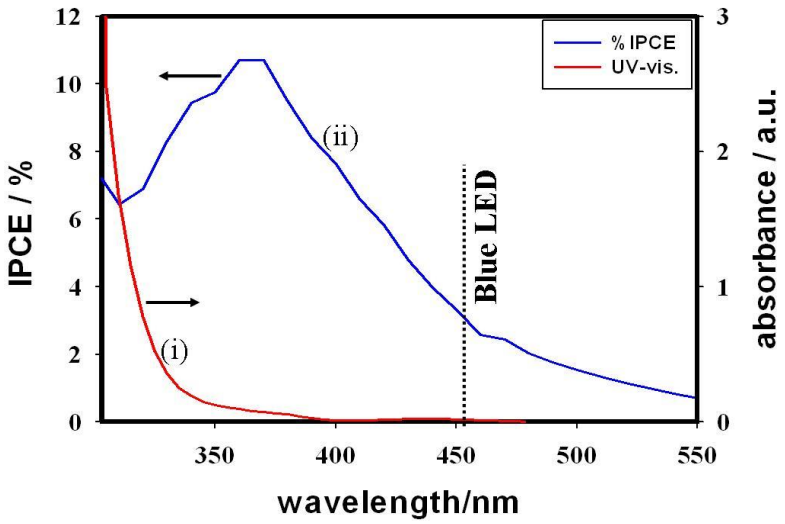

Figure 3 (i) Absorption spectrum (in air) of 3STF film electrodes (ITO electrode background subtracted). (ii) IPCE measurement for 3STF (EE) film electrode immersed in 1 M NaOH and with a +0.7 V vs. Ag/AgCl applied potential.

The absorption coefficient of the STF film can only be estimated. In the wavelength region around 380 nm the onset of the absorption is observed and the absorbance is approximately A = 0.058 (Figure 3i). The extinction coefficient can be estimated based on

$$\alpha = \frac{A}{2.3\,l} = 21928\ m^{-1} \qquad (2)$$

where *l* is the thickness of the STF film (ca. 1.15 μm). The real absorption coefficient could be considerably lower than this estimated value due to additional losses from poor optical coupling and light scattering. It was observed that the absorption is slightly higher in case of illumination via the EE side compared to that in case of illumination via the SE side as it was discussed in the previous. It was observed that the absorption is slightly higher in case of illumination via the EE side compared to that in case of illumination via the SE side as it was discussed in the previous chapters. Ideally, the cells will absorb as much of the blue region of the spectrum with a high overall incident photon to current efficiency. It has been found that the peak "Incident Photon Conversion Efficiency" or IPCE (Figure 3) is at approximately 380 nm. Therefore a scan range of 550 nm to 300 nm was chosen to investigate the efficiency of the STF cell. A comparison between the efficiency of SE illumination and that on EE shows that the difference between the IPCE of EE side and that if SE side are not that high. This might be due to the fact that the films are not thick. It was found also that the efficiency increases slightly with increase in film thickness (Hassan, 2015), as in Figure 4 (the thickness is not shown but sample 2STF is thicker than sample 3STF). The IPCE data suggest good photoelectrochemical activity (although not quite as good as the silica-doped materials). Further improvements are likely when the effects of thickness and calcination temperature are studied in more detail.

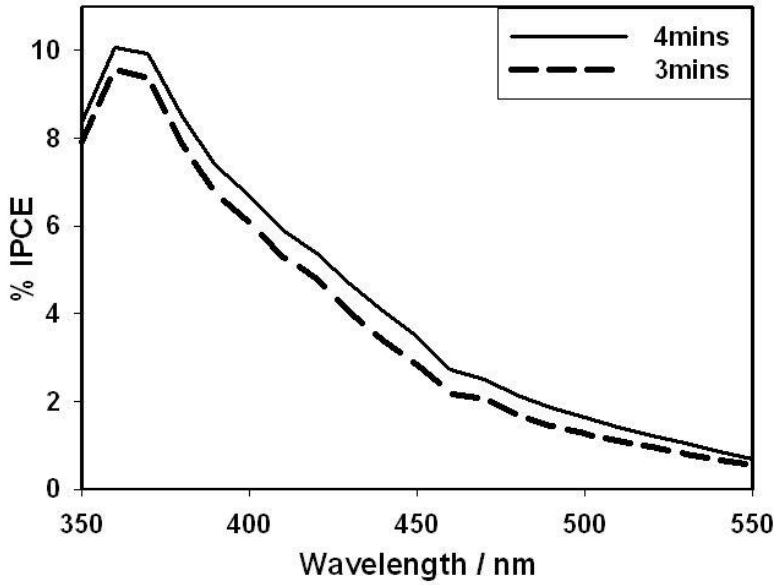

Figure 4. Comparison of %IPCE of samples 3STF and 2 STF deposited by spray pyrolysis on ITO for 3 and 4 minutes, respectively, immersed in 1 M NaOH at applied potential 0.7V vs. Ag/AgCl, illuminated by xenon lamp through SE side. The thickness is not shown here but sample 2STF is thicker than sample 3STF

3.2 Electrochemical Impedance Spectroscopy

Impedance methods can be employed to provide time scale (or frequency domain) dependent information about reactions and processes. Here, the impedance measurements were taken for STF

samples prepared by using the spray pyrolysis method. Figure 5 shows data for the dark impedance for a STF film (3STF) obtained at a range of applied potentials (0.0 to 0.7 V vs. Ag/AgCl) in aqueous 1 M NaOH. In zeroth approximation, impedance data can be modelled based on the Randles circuit or equivalent circuit (Figure 5) with a "short" Warburg element to represent a thin film of redox active material. R1 and C represent the dominating cell resistance and interfacial capacitance. As expected, by increasing the applied positive potential, a decrease in impedance was observed (more current could flow). The impedance data can be approximately modelled when assuming the Randles circuit with "open" Warburg element. The physical significance of this observation is associated with the electron transfer at the film/electrode interface, which might lead to formation of higher oxidation states of Fe (IV/V/VI) and the resulting water spitting reaction causing higher or "catalytic" currents.

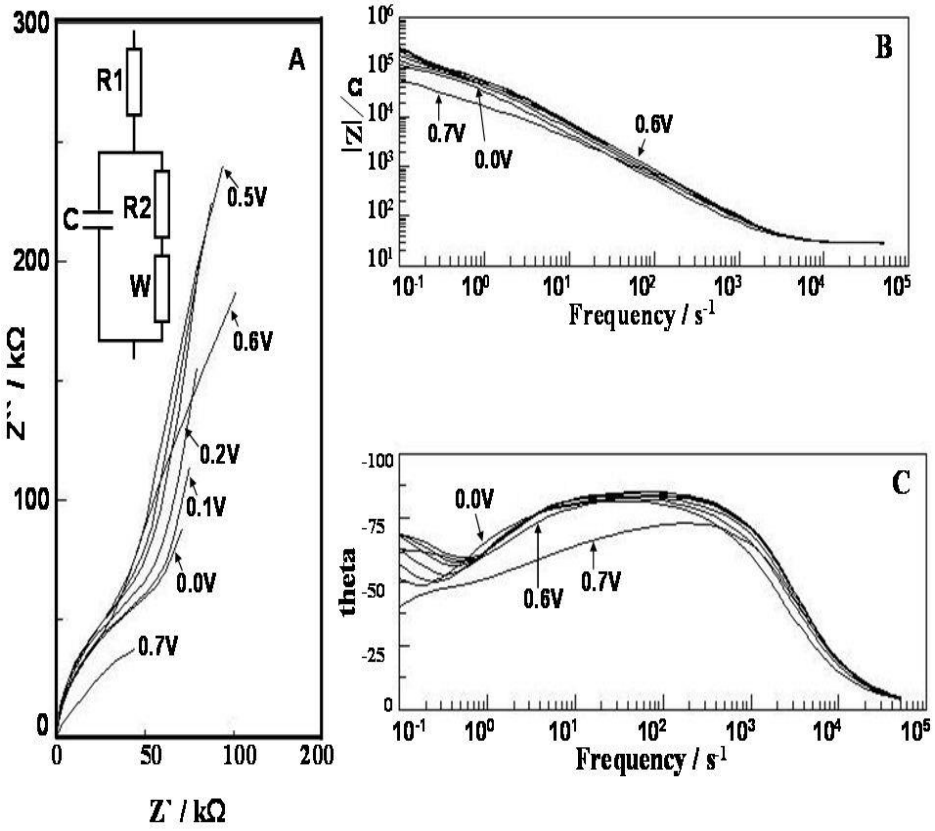

Figure 5 (A) Nyquist plots and (B, C) Bode plots for the effect of different applied (DC) potentials on the dark impedance for 3STF film electrode in 1 M NaOH (potentials in V vs. Ag/AgCl. The inset (up left) shows the equivalent circuit which has been used.

It was also found that, in the presence of light, additional currents caused a further decrease of the impedance consistent with a faster light energy driven water splitting reaction. Figure 6 represents the Nyquist plots (A) and Bode plots (B, C as inset) of impedance results under illumination of sample 3STF (spraying time, 3 min) through SE side by using blue LED (455 nm) at light intensity corresponding to 300 mA (10.09 mW cm^{-2}). By increasing the applied positive potential the

impedance dramatically decreased as at potentials 0.4 V to 0.7 V in comparison to data at lower positive potentials 0.0 V to 0.3 V (Figure 6 A). This confirms high photocurrent transients at higher applied positive potentials.

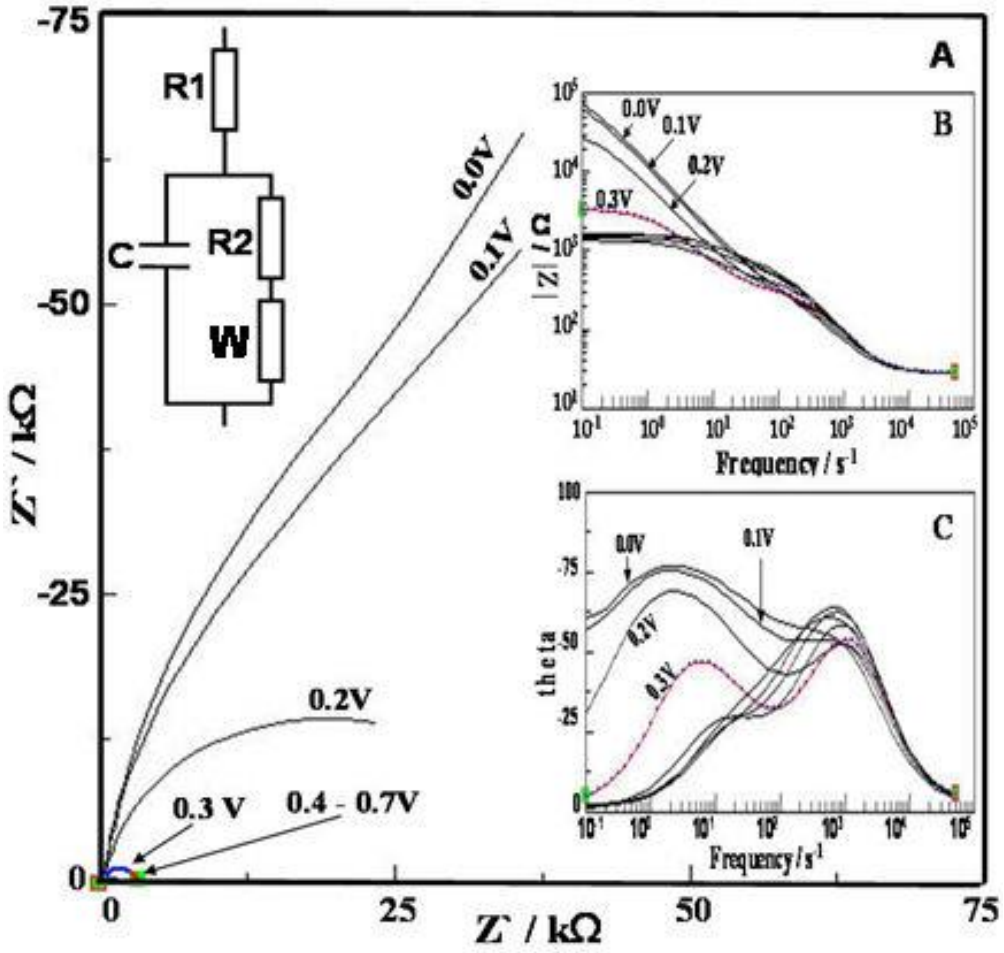

Figure 6. (A) Nyquist plots and (B, C as inset) Bode plots for the effect of SE illumination at different applied (DC) potentials (0.0 - 0.7V) on the impedance for 3STF film (3 minutes spraying time) electrode in 1 M NaOH (potentials in V vs. Ag/AgCl). The inset (up left) shows the equivalent circuit which has been used. The impedance resulted after application of potentials 0.4- 0.7 V are hidden in the left bottom corner because they are very small in comparison to the impedance resulted by application of lower potentials (0.0 - 0.3 V).

For more illustration for the effect of illumination on the obtained impedance results, a comparison between the dark impedance and that under illumination through SE side using blue LED at 10.09 mWcm2 light intensity is shown in Figure 7.

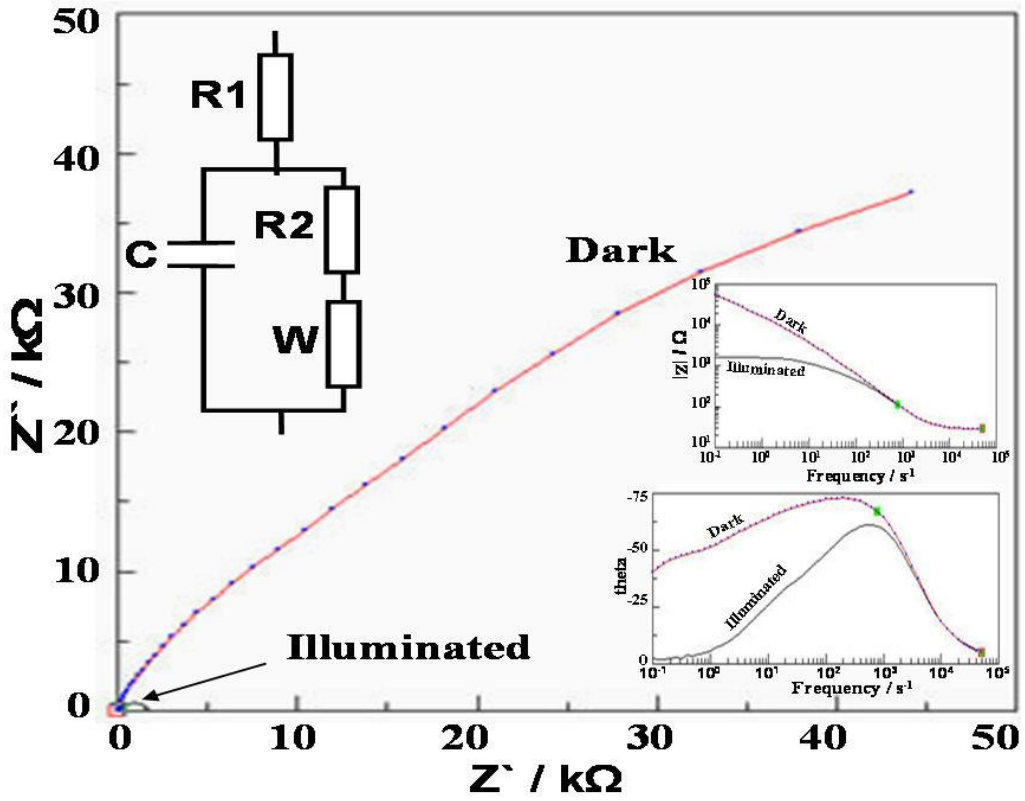

Figure 7. A: Nyquist plots and (B, C as inset) Bode plots for the effect of SE illumination at 0.7 V applied (DC) potentials on the impedance for 3STF film (3 minutes spraying time) electrode in 1 M NaOH (potentials in V vs. Ag/AgCl. The inset (up left) shows the equivalent circuit which has been used.

Figure 8 represents the comparison between the dark impedance of sample 3STF (spraying time, 3 min) and that of sample 2STF (spraying time, 4 min) in 1 M NaOH at applied potential 0.7V vs. Ag/AgCl. It was found that by increasing the spraying time (thickness) the impedance decreases at all applied potentials. The impedance method provides some additional insight via parameterization in terms of resistances and capacitances. However, for further insight in to the mechanism and potential applicability of STF films in photo-electrochemical devices a wider range of thicknesses and a wider range of compositions needs to be studied.

All impedance data obtained from the application of the Randles circuit, as it is shown in the above Figures, for dark and illuminated impedance for sample 3STF (spraying time, 3 min) and that of dark and illuminated impedance of sample 2STF (spraying time, 4 min) are shown in Tables 2 and 3. In dark impedance both of resistance and capacitance are slightly decreasing with increasing the applied potential from 0.0 to 0.7V vs. Ag/AgCl. The same behaviour has been noticed by illuminations through EE side, in case of sample 2STF and on both SE and EE sides in case of sample 3STF (see Tables 2 and 3). The resistance reported in the Tables 2 and 3 are mainly the ITO

substrate resistance in addition to that of the electrolyte (which is tiny in comparison to that of the substrate).

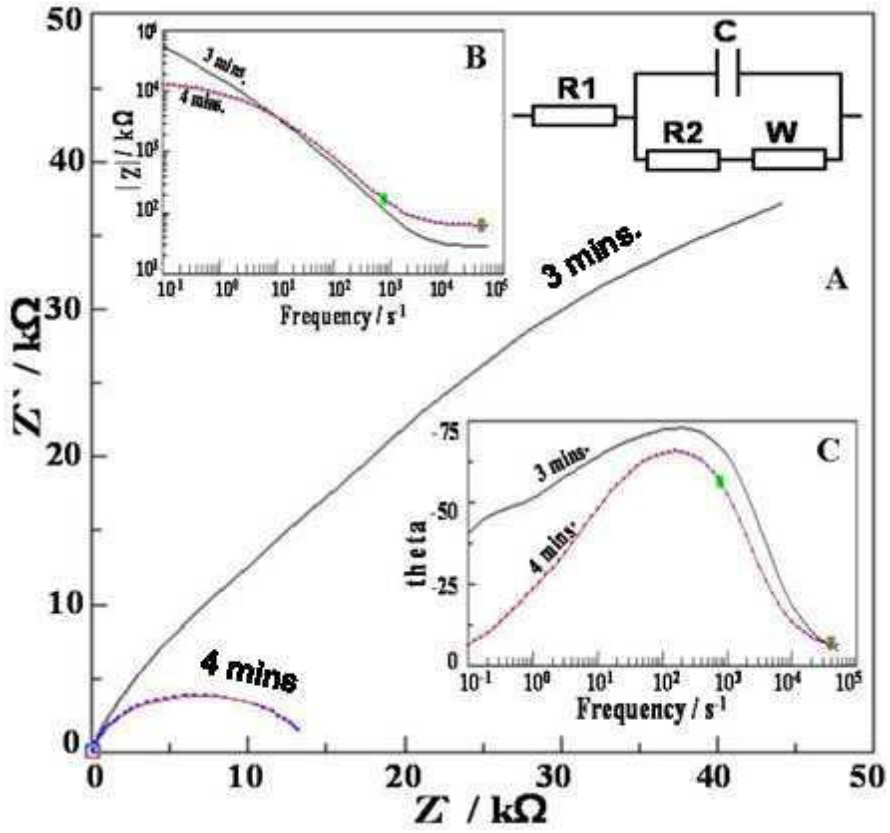

Figure 8. (A) Nyquist plots and (B, C as inset) Bode plots for the effect of sample thickness or spraying time (3 and 4 minutes spraying time for samples 3STF and 2 STF films respectively) on dark impedance of STF samples at 0.7 V applied (DC) potential vs. Ag/AgCl in 1 M NaOH (potentials in V vs. Ag/AgCl. The inset (top right) shows the equivalent circuit which has been used.

Table 2. Impedance data for a spray-pyrolysed 3STF film (3 minutes spraying time) on ITO (area 0.38 cm^2) and immersed in aqueous 1 M NaOH at different applied DC potentials and at 10 mV AC amplitude (light source: blue LED at light intensity 300 mA (10.09 mW cm^{-2}).

E / V *vs.* Ag/AgCl	Conditions		*R* / Ω [a]	*C* / μF [a]
0.0	Dark		30.3	2.68
	Light	EE	**27.56**	**1.96**
		SE		
	Dark		29.8	2.14

0.1	**Light**	**EE**	**38.31**	**4.33**
		SE		
0.2	**Dark**		29.35	1.87
	Light	**EE**	**38.31**	**4.33**
		SE		
0.3	**Dark**		29.02	1.72
	Light	**EE**	**35.61**	**3.28**
		SE		
0.4	**Dark**		29.13	1.81
	Light	**EE**	**35.44**	**3.21**
		SE	**27.42**	**1.72**
0.5	**Dark**		28.95	1.78
	Light	**EE**	**35.23**	**3.17**
		SE	**27.92**	**1.79**
0.6	**Dark**		28.39	1.65
	Light	**EE**	**35.39**	**3.21**
		SE	**28.28**	**1.83**
0.7	**Dark**		28.68	1.73
	Light	**EE**		
		SE	**29.03**	**2.10**

[a] *parameters obtained by employing the "fit circle" option in Zview.*

Table 3. Impedance data for a spray-pyrolysed 2STF film (4 minutes spraying time) on ITO (area 0.38 cm^2) and immersed in aqueous 1 M NaOH at different applied DC potentials and at 10 mV AC amplitude (light source: blue LED at light intensity 300 mA (10.09 $mW.cm^{-2}$).

E **/ V *vs.* Ag/AgCl**	**Conditions**		***R*** **/Ω** [a]	***C*** **/ µF** [a]
0.0	**Dark**		65.42	1.94
	Light	**EE**	**63.42**	**9.57**
		SE	**64.03**	**5.40**

0.1	**Dark**		64.28	1.47
	Light	**EE**	**63.09**	**8.66**
		SE	**56**	**2.57**
0.2	**Dark**		63.64	1.30
	Light	**EE**	**62.79**	**7.71**
		SE	**56.04**	**2.85 x 10^{-8}**
0.3	**Dark**		63.46	1.24
	Light	**EE**	**62.83**	**7.63**
		SE	**59.57**	**8.85 x 10^{-3}**
0.4	**Dark**		63.38	1.21
	Light	**EE**	**62.82**	**7.56**
		SE	**63.94**	**4.70**
0.5	**Dark**		63.81	1.26
	Light	**EE**	**63.10**	**8.64**
		SE	**64.28**	**4.78**
0.6	**Dark**		63.55	1.23
	Light	**EE**	**62.48**	**8.24**
		SE	**64.38**	**4.95**
0.7	**Dark**		66.3	1.62
	Light	**EE**	**72.83**	**5.94**
		SE	**62.34**	**4.15**
0.8	**Dark**		70.96	2.34
		EE		
		SE		

[a] *parameters obtained by employing the "fit circle" option in Zview.*

4. Conclusion

Incident Photon to Current Efficiency, UV-vis absorption spectrometry and electrochemical impedance spectroscopy measurements have been performed successfully on strontium titanate ferrate (STF) solid solution for solar energy conversion applications. The STF samples were prepared spray pyrolysis approach on ITO substrates, at high temperature. In general, the proposed nanostructured STF films exhibited high photocurrent response, with IPCEs of up to 11%, and high absorption of UV-visable light in air, in the wavelength range 300 to 400 nm. The IPCE increases slightly with increase in the film thickness, and the impedance increases with increase in the applied potential and decreases with the increase in film thickness. The current study demonstrates that

Iron oxides with substitution of metal sites give rise to a family of materials with solid solution character, known as Perovskite family AMO_3. This opens up new opportunities for solid solutions as "tuneable" photoanodes, which can be used as a main photosystem for example in the tandem cell to split water by using solar radiations. A lot more work will be necessary to develop and characterize these types of materials in the future.

Acknowledgements

The author would love to thank Professor Laurie M. Peter and Professor Frank Marken, at Department of Chemistry, University of Bath, Bath, UK, for their kind help during this work. Many thanks to Dr. Gabriele Kociok-Köhn in the Department of Chemistry, University of Bath, Bath, UK for XRD measurements. The author would also like to thank Mr. Hugh Perrott and Dr. John M. Mitchels in the Department of Physics, University of Bath, Bath, UK, for SEM and EDX measurements. Finally, the author expresses deepest gratitude to the Egyptian Government for funding.

References

Adler, P, Eriksson S. (2000). Structural Properties, Mössbauer Spectra, and Magnetism of Perovskite-Type Oxides $SrFe_{1-x}Ti_xO_{3-y}$. Zeitschrift für anorganische und allgemeine Chemie. 626(1): 118-124.

Brixner, LH. (1968). Preparation and properties of the $SrTi_{1-x}Fe_xO_{3-x^2}/O_{x^2}$ system. Materials Research Bulletin. 3(4): 299-308.

Hassan, IAI. (2015). Development and Characterization of Novel Nanostructured $SrTi_{1-x}Fe_xO_{3-y}$ solid solution for Solar Electricity Generation. International Journal of Advanced Thermofluid Research. 1(1): 17-27.

Krishnan, RR, Vinodkumar, R, Rajan, G, Gopchandran, KG, Pillai, VPM. (2010). Structural, optical, and morphological properties of laser ablated ZnO doped Ta_2O_5 films. Materials Science and Engineering: B. 174(1-3): 150-158.

Langford, JI, Wilson, AJC. (1978). Scherrer after sixty years: A survey and some new results in the determination of crystallite size. Journal of Applied Crystallography. 11(2): 102-113.

Rothschild, A, Menesklou, W, Tuller, HL, Ivers-Tiffée, E. (2006). Electronic Structure, Defect Chemistry, and Transport Properties of $SrTi_{1-x}Fe_xO_{3-y}$ Solid Solutions. Chemistry of Materials. 18(16): 3651-3659.

Rothschild, A. and H. Tuller (2006). Gas sensors: New materials and processing approaches. Journal of Electroceramics. 17(2-4): 1005-1012.

Shilova, YA, Patrakeev, MV, Mitberg, EB, Leonidov, IA, Kozhevnikov, VL, Poeppelmeier, KR. (2002). Order–disorder enhanced oxygen conductivity and electron transport in Ruddlesden–Popper ferrite-titanate $Sr_3Fe_{2-x}Ti_xO_{6+\delta}$. Journal of Solid State Chemistry. 168(1): 275-283.